Water Air Soil Pollut (2026) 237:528
https://doi.org/10.1007/s11270-026-09235-4

Potential of Physical Activated Carbon Derived from Pyrolyzed Waste Coffee Grounds as an Adsorbent for Dye Removal

Mirac Nur Ciner · Emine Elmaslar Özbaş · Huseyin Kurtuluş Ozcan · Atakan Ongen

Received: 18 September 2025 / Accepted: 4 February 2026
© The Author(s) 2026

Abstract This study investigates the adsorption performance of activated carbon prepared from spent coffee grounds (SCG) through pyrolysis and subsequent CO_2-assisted physical activation for the removal of Methylene Blue (MB) dye from aqueous solutions. SCG was pyrolyzed at 400 °C, 500 °C, and 600 °C, and the resulting biochars were activated at 900 °C under CO_2 flow. The obtained materials were characterized using FTIR, SEM, BET, and elemental analyses to evaluate structural, morphological, and chemical properties. Among the samples, the activated carbon derived from 600 °C pyrolysis exhibited the highest surface area (44.59 m^2/g) and was selected for detailed adsorption studies. Batch experiments were conducted to investigate the influence of pH (4–9), adsorbent dosage (2.5–15 g/L), initial dye concentration (15–50 mg/L), temperature (10–40 °C), and contact time (0–120 min) on MB removal efficiency. The maximum removal efficiency (99.15%) was obtained at 15 g/L and 45 min, while comparable performance (> 98.9%) was achieved even at lower dosages, indicating high adsorption capacity and economic feasibility. Kinetic analysis revealed that the adsorption process followed the pseudo-second-order model ($R^2 > 0.94$). The Freundlich isotherm ($R^2 = 0.9924$) provided the best fit, indicating multilayer adsorption on heterogeneous surfaces. These findings demonstrate that SCG-derived activated carbon is an effective, sustainable, and low-cost adsorbent with strong potential for dye removal and wastewater purification. The study also highlights the environmental value of coffee waste valorization within a circular economy framework, contributing to resource recovery and sustainable material development.

Keywords Activated Carbon · Waste Coffee Grounds · Pyrolysis · Adsorption · Dye Removal · Methylene Blue

M. N. Ciner (✉) · E. E. Özbaş · H. K. Ozcan · A. Ongen
Engineering Faculty, Environmental Engineering Department, Istanbul University-Cerrahpaşa, Avcılar, Istanbul, Türkiye
e-mail: mirac.ciner@iuc.edu.tr

E. E. Özbaş
e-mail: elmaslar@iuc.edu.tr

H. K. Ozcan
e-mail: hkozcan@iuc.edu.tr

A. Ongen
e-mail: aongen@iuc.edu.tr

1 Introduction

Coffee *(Coffea spp.)* is one of the most widely consumed beverages globally and is derived from tropical plants of the Rubiaceae family (Deribe, 2019). Coffee beans, rich in phenolic compounds, melanoidins, and diterpenes, retain a substantial amount of bioactive content even after brewing (Rufián-Henares & Pastoriza, 2015). The residual product, known as spent coffee grounds (SCG), remains rich in organic

Published online: 09 February 2026

compounds including fatty acids, lignin, cellulose, hemicellulose, and polysaccharides (Thenepalli et al., 2017). With growing global demand for coffee, large amounts of SCG are produced and often discarded as municipal waste. For example, in 2018, Turkey's coffee consumption reached 93.9 thousand tons, with per capita intake exceeding 1.1 kg for the first time (ICO, 2018). Globally, more than 50% of the coffee mass is disposed of during processing, creating a substantial volume of waste with environmental implications due to the presence of bioactive and phytotoxic compounds such as caffeine, tannins, and polyphenols (Esquivel & Jiménez, 2012; Mata et al., 2018).

Unlike other organic wastes, SCG are not easily compostable due to their potential toxicity to microorganisms, making them unsuitable for traditional biological treatment methods. Consequently, they are typically managed via landfilling, which poses both ecological and economic burdens (McNutt, 2019). However, the high organic content and porous structure of SCG make them a promising raw material for the synthesis of value-added products. Several studies have investigated the use of SCG in applications such as biofuel production, composting enhancement, and material development (Bomfim et al., 2022; Karmee, 2018; Yusufoğlu et al., 2024). Among these, the conversion of SCG into activated carbon through pyrolysis stands out due to its ability to transform a problematic waste into a functional, high-surface-area adsorbent suitable for environmental applications (Ciner et al., 2024a; Murthy & Naidu, 2012; Setter et al., 2020).

Recent research has increasingly focused on transforming biomass wastes such as citrus peels, nutshells, and agricultural residues into porous carbons with high adsorption potential for dyes and heavy metals. For instance, Akkaya Sayğılı et al. (2020) produced activated carbon from mixed citrus fruit wastes via H_3PO_4 activation, achieving a surface area exceeding 1000 m^2/g and demonstrating efficient Pb (II) removal through Langmuir-type adsorption behavior. Similarly, Sayğılı and Güzel (2018a, 2018b-a) and Güzel et al. (2021) emphasized the role of activation conditions and precursor composition in tailoring pore structure and surface functionality, which directly influence adsorption kinetics and thermodynamics. Similar trends were observed for mesoporous activated carbons obtained by CO_2 or steam activation, which showed efficient removal of dyes such as Congo Red mainly through physisorption (Sayğılı & Güzel, 2018a, 2018b-b). These findings support the feasibility of using low-cost biomass precursors to develop high-efficiency adsorbents with circular-economy relevance. Building on these findings, the valorization of coffee waste represents an underexplored yet promising route toward sustainable material production.

Among these materials, SCG stand out as a promising precursor for high-quality activated carbon. SCG possesses a high fixed carbon content, moderate volatile matter, and abundant oxygenated surface groups derived from lignocellulosic polymers such as cellulose, hemicellulose, and lignin, which decompose during pyrolysis to form a highly carbonaceous and reactive matrix (Campos-Vega et al., 2015). These intrinsic characteristics promote pore formation, enhance surface functionality, and improve adsorption affinity toward polar pollutants such as dyes. SCG are known to contain significant lipid content in addition to cellulose, hemicellulose, and lignin, which may contribute to pore development and surface activation during pyrolysis (Ahmed et al., 2024). Compared to other biomass residues, SCG has a uniform particle size, low ash content, and consistent composition, allowing for reproducible and high-quality activated carbon production (Johnson et al., 2022).

Commercial activated carbon (CAC) is commonly used as a reference adsorbent for dye removal owing to its high surface area (800–1500 m^2/g) and methylene blue (MB) adsorption capacities often exceeding 200 mg/g (Bansal & Goyal, 2005). However, its widespread application is constrained by high production costs, energy-intensive processes, and dependence on non-renewable resources.

Chemically activated or chemically treated materials derived from SCG have been reported to exhibit enhanced adsorption performance for organic dyes due to improved surface chemistry and porosity. Alkali and acid treatments, such as KOH and H_3PO_4 or HNO_3 modification, significantly increase MB adsorption capacity by introducing oxygen-containing functional groups (Araya-Sibaja et al., 2025). Similarly, KOH chemical activation of SCG produces highly porous carbon materials with large surface areas and superior dye adsorption capacities, highlighting the effectiveness of alkali activation for SCG-based adsorbents (Sukhbaatar et al., 2021).

Despite their high performance, chemical activation routes involve corrosive reagents, extensive post-treatment, and secondary wastewater generation, raising environmental and economic concerns. In contrast, physical activation using CO_2 or steam is considered a more environmentally benign alternative for biomass-derived carbons, as it avoids the use of corrosive chemical agents and reduces secondary pollution associated with chemical activation processes (Ioannidou & Zabaniotou, 2007). Although physically activated carbons generally exhibit lower surface areas, adsorption performance in dye removal systems is strongly influenced by surface functional groups and pore accessibility rather than surface area alone.

However, despite these advances, relatively few studies explicitly frame SCG-derived activated carbon production within a circular-economy or waste-valorization context, representing a distinct research gap (Al Balushi et al., 2025; Ciner et al., 2024a; Ciner et al., 2024b). Existing works often emphasize activation methods or adsorption efficiency, yet lack a comprehensive sustainability assessment integrating resource recovery principles.

The novelty of this study lies in its dual emphasis on material functionality and sustainability: SCG grounds are utilized not only as a precursor for activated carbon but also as a means of promoting resource-efficient utilization (Shah et al., 2025). This approach directly aligns with the goals of the circular economy by minimizing waste generation and reducing dependence on virgin materials.

One of the most critical environmental applications of activated carbon is the removal of synthetic dyes from wastewater. Dyes discharged by textile, leather, and paper industries are often highly stable, toxic, and non-biodegradable, even at low concentrations. Traditional treatment technologies such as chemical oxidation, precipitation, and membrane filtration often suffer from high operational costs or low effectiveness (Ahmad et al., 2015). Adsorption, on the other hand, is considered one of the most practical and efficient techniques for dye removal when appropriate adsorbents are used (Özbaş et al., 2013, 2019). Activated carbon, with its high porosity, large surface area, and favorable surface chemistry, has been extensively studied for its ability to adsorb a wide range of pollutants.

By adopting a circular approach, this research couples the pyrolytic valorization of SCG grounds with dye adsorption applications, demonstrating an integrated pathway for waste reduction and environmental remediation. Through this integration, the study contributes to both wastewater treatment innovation and sustainable material management.

The present study aims to evaluate the potential of activated carbon derived from SCG grounds for the adsorption of MB dye from aqueous solutions. Within this scope, SCG was subjected to pyrolysis and physical activation, and the resulting materials were thoroughly characterized using standard analytical techniques. The adsorption behavior of the activated carbon was investigated under varying experimental conditions, including initial pH, dye concentration, contact time, adsorbent dosage, and temperature. Additionally, kinetic and equilibrium models were applied to interpret the adsorption mechanism, and thermodynamic parameters were assessed to understand the nature of the process. Through this approach, the study provides a detailed assessment of the applicability of SCG-based activated carbon for dye removal in water treatment processes.

2 Kinetic Studies

Various kinetic models are utilized to interpret the behavior of the adsorbent, determine the controlling mechanism of the adsorption process, and evaluate the experimental data. In this study, the adsorption behavior was assessed using two kinetic approaches: the pseudo-first-order and pseudo-second-order models. The agreement between the experimental results and the predicted values from these models was determined using the coefficient of determination (R^2). A higher R^2 value indicates a better fit of the model to the dye adsorption kinetics. The pseudo-first-order model was originally proposed by Lagergren (Ho, 2016; Khezami et al., 2016; Rodrigues & Silva, 2016; Rudzinski & Plazinski, 2007).

A pseudo-first-order equation can be expressed in a linear form (Eq. 1):

$$log\left(q_e - q_t\right) = log\left(q_e\right) - \left(k_1/2.303\right)t \quad (1)$$

where q_e and q are the amounts of dye adsorbed (mg/g) on the adsorbents at the equilibrium and

at time t, respectively, and k_1 is the rate constant of adsorption (min^{-1}). Values of k_1 were calculated from the plots of $\log(q_e - q_t)$ versus t for different concentrations of the basic dye.

The sorption data was also analyzed in terms of pseudo-second-order mechanism described in Refs. (Suteu et al., 2016; Prandini et al., 2022):

The pseudo-second-order adsorption kinetic rate equation is expressed as follows (Eq. 2):

$$dq_t/dt = k_2\left(q_e - q_t\right)^2 \quad (2)$$

where k_2 is the rate constant of pseudo-second-order adsorption (g/mg min). Integrating and applying the initial conditions, the equation can be presented as linear form (Eq. 3):

$$t/q_t = \left[1/\left(k_2 q_e^{\,2}\right)\right] + \left(1/q_e\right)(t) \quad (3)$$

where q_e is the amount of dye adsorbed at equilibrium (mg/g). The second-order rate constants were used to calculate the initial sorption rate, $h = k_2 q_e^{\,2}$.Values of k_2 and q_e were calculated from the intercept and the slope of the linear plots of t/q_t versus t.

3 Adsorption Isotherms

Langmuir and Freundlich equations are commonly used in the adsorption isotherm studies. The Langmuir theory assumes that sorption takes place at specific sites within the adsorbent, which means that no further adsorption can take place at a site occupied by a dye molecule. Therefore, the saturation monolayer can be then represented by the following expression (Eq. 4) (Guo & Wang, 2019; Zhang et al., 2025):

$$\left(C_e/q_e\right) = \left(1/q_m K\right) + \left(1/q_m\right)C_e \quad (4)$$

where q_m is the maximum amount of adsorption (mg/g), K is the affinity constant (L/g) and C_e is the solution concentration at equilibrium (mg/L).

The Freundlich model assumes that the sorption takes place on heterogeneous surfaces and adsorption capacity depends on the concentration of dyes at equilibrium. The well-known logarithmic form of Freundlich model is given by the following equation (Eq. 5) (Joshi et al., 2023; Wang et al., 2023):

$$Inq_e = InK_F + (1/n)InC_e \quad (5)$$

where K_F and n are the Freundlich constants related to the adsorption capacity and adsorption intensity, respectively.

The Temkin isotherm equation assumes that the heat of adsorption of all the molecules in the layer decreases linearly with coverage due to adsorbent-adsorbate interactions, and that the adsorption is characterized by a uniform distribution of the bonding energies, up to some maximum binding energy (Lee, 2020; Xia et al., 2006). The Temkin isotherm is given as:

$$qe = BInA + BInCe \quad (6)$$

where A (l/g) is the equilibrium binding constant, corresponding to the maximum binding energy. A plot of qe versus lnCe enables the determination of the isotherm constants B and A from the slope and intercept of the straight line plot., and constant B is related to the heat of adsorption.

In this study, the effect of adsorbent amount, dye concentration, contact time and pH on the removal of synthetic MB dye by activated carbon adsorption from SCG was investigated. At the hands of activated carbon; physical activation methods have been used.

4 Material And Method

4.1 Biochar Preparation

The SCG used in this study was sourced from a local coffee shop and initially dried in a Memmert-brand oven at 50 °C for a duration of 48 h. Subsequently, biochar was produced from the dried SCG through pyrolysis, and both the raw material and the generated biochar were subjected to characterization analyses. Prior to the pyrolysis process, the SCG samples underwent an additional drying phase at 50 °C to ensure moisture minimization. Approximately 50 g of the dried SCG were loaded into a fixed-bed steel reactor, featuring an internal diameter of 8 cm and an approximate volume of 3 L. The reactor's heating rate was regulated using an electrical control panel, and thermal insulation was provided by rock wool to reduce heat loss. To ensure an inert atmosphere during pyrolysis, nitrogen gas (N_2) was continuously introduced into the system at a constant flow rate of about 1.0 L/min. The pyrolysis was carried out for

4 h at a predetermined temperature. In order to prevent gas leakage from the reactor, pure graphite and graphite-lead spiral gaskets were employed to ensure sealing integrity.

The reactor system was designed with a gas inlet line for the continuous introduction of N_2 and an outlet line located on the reactor lid to facilitate the discharge of synthesis gases. Throughout the experimental process, the internal temperature of the reactor was precisely monitored using a thermocouple. To condense the volatile organic compounds released during pyrolysis, two sequential cooling columns were employed; the resulting condensates were collected in conical flasks positioned at the base of each column. The non-condensable fraction of the synthesis gas was directed to a gas analyzer to assess its composition. To protect the analyzer from potential damage caused by uncondensed volatile organics and particulate matter, the gas outlet line was equipped with one ceramic filter and two microfiber filters. Pyrolysis experiments were conducted under controlled laboratory conditions at target temperatures of 400 °C, 500 °C, and 600 °C, with a heating rate of approximately 20 °C/min. The schematic representation of the pyrolysis setup is provided in Fig. 1.

4.2 Physical Activation

In order to increase the specific surface area of the biochar produced via pyrolysis, a physical activation process was applied. This was achieved by introducing CO_2 gas into the same reactor used during pyrolysis, maintaining a temperature of 900 °C for a duration of 4 h. The activation temperature of 900 °C was selected because studies have shown that higher activation temperatures ($\geq$850 °C) enhance micropore formation and BET surface area by promoting volatile removal and carbon structure reorganization. In particular, Phothong et al. (2021) and Azargohar and Dalai (2008) reported that activation between 850–950 °C leads to well-developed porosity and

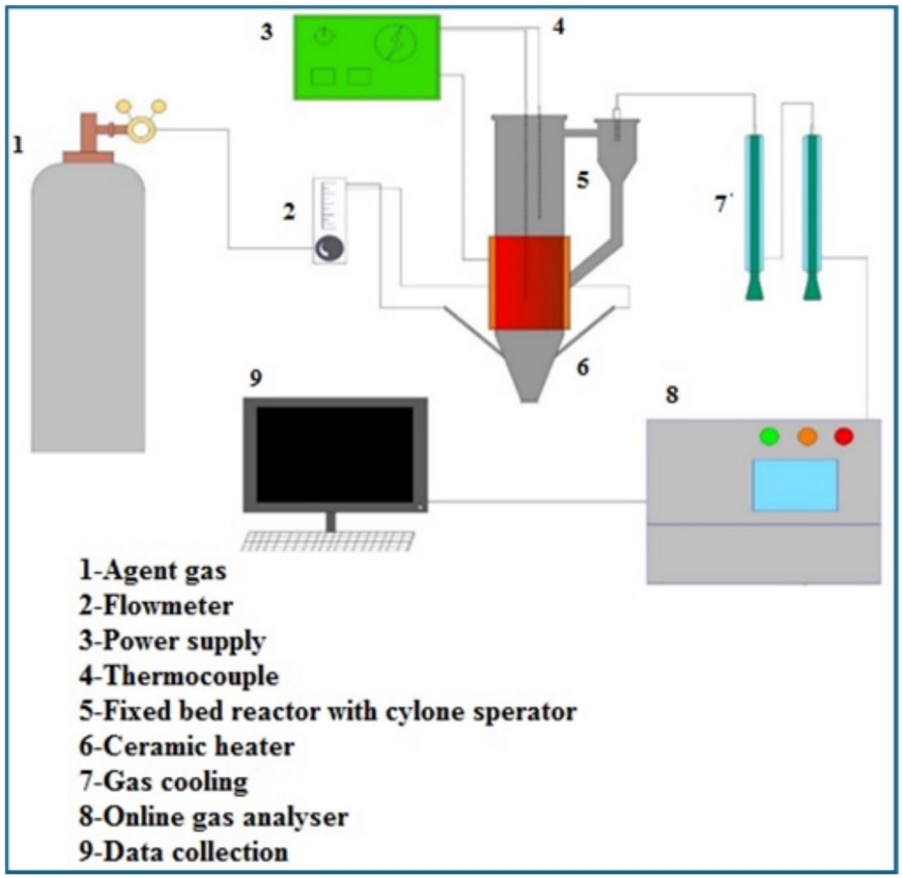


Fig. 1 Experimental setup used for the pyrolysis

optimal adsorption performance, while temperatures above this range cause structural degradation. Thus, 900 °C was chosen as the optimum temperature to maximize pore development without excessive carbon loss.

An activation duration of 4 h was chosen as an optimal compromise between surface area enhancement and carbon yield. Studies have shown that extending activation beyond this period can cause excessive burn-off and pore collapse, reducing adsorbent integrity. Nogueira et al. (2025) and Hsi et al. (2011) both reported that while longer activation times initially increase surface area, prolonged exposure leads to structural degradation and yield loss.

4.3 Analytical Methods

Comprehensive physical and chemical characterizations were conducted on both the biochar derived from pyrolysis and the physically activated biochar obtained thereafter. All analytical procedures were performed in accordance with American Society for Testing and Materials (ASTM) standard methodologies, as outlined in Table 1. To ensure the reliability and reproducibility of the results, each analysis was carried out in triplicate.

4.4 Moisture Content and Solids Content

The determination of total moisture and solid content in solid fuel samples was performed using the standard oven-drying method. The samples were placed in crucibles and dried in a Memmert-brand oven at 105 °C until a constant weight was achieved, typically within approximately one hour. Subsequently, the moisture and solid content percentages were calculated using Eqs. (7) and (8), respectively.

$$WeightMoisture(\%) = \frac{(A-B)}{A} \times 100 \quad (7)$$

$$WeightSolids(\%) = \left(\frac{B}{A}\right) \times 100 \quad (8)$$

Here,
A = First test sample, g
B = Dried test sample, g

4.5 Combustion Loss and Ash Content

Ash content determination is a widely applied analytical method used to quantify the total mineral or inorganic content within a material. Ash refers to the non-combustible residue that remains following the complete combustion of the sample's organic constituents. In this procedure, the samples are placed in ceramic crucibles and subjected to thermal treatment at 550 °C for 120 min. Following combustion, the furnace is allowed to cool to 105 °C. The ash content and combustion loss are then calculated using Eqs. (9) and (10). This analysis was performed using a Magma Therm Primary MTP Series Furnace, Model No. MTP-1000–8-P.

$$WeightLossonCombustion(\%) = \frac{(A-B)}{A} \times 100 \quad (9)$$

$$WeightAshContent(\%) = \left(\frac{B}{A}\right) \times 100 \quad (10)$$

Here,
A = First test sample, g
B = Dried test sample, g

4.6 Calorific Value Analysis

The calorific value of the samples was determined using an IKA C200 bomb calorimeter, which evaluates

Table 1 Technical standards for characterization

Technical Standards	Analysis type
ASTM D-3173	Determination of Moisture Content and Solids Content
ASTM D-3174	Determination of Loss on Burning and Ash Content
ASTM D-5865	Determination of Calorific (Thermal) Value
ASTM D-5373	Elemental analysis
ATSM E-1252	Fourier Transform Infrared Spectrometer (FTIR)

the higher heating value (HHV) of solid fuels. The combustion process was carried out in a sealed vessel under a pressurized oxygen-rich environment (30 bar), fully immersed in a known volume of water. Each sample, enclosed in a plastic bag and placed in a quartz crucible, was ignited using a cotton thread attached to an ignition electrode. The resultant temperature rise in the surrounding water (ΔT) was recorded, and the HHV was calculated on a wet basis accordingly.

4.7 Elemental Analysis

This analytical approach offers detailed information on the elemental composition of the samples, focusing primarily on carbon (C), hydrogen (H), and nitrogen (N) content. Such analyses are typically carried out using combustion-based techniques or instrumental methods involving elemental analyzers. In the present study, elemental analysis was performed using the Thermo Scientific Flash Smart 2000 instrument.

4.8 Fourier Transform Infrared Spectroscopy (FTIR)

Fourier Transform Infrared Spectroscopy (FTIR) is an analytical technique utilized to investigate both organic and inorganic substances by identifying their chemical bonds and molecular structures (Lopes et al., 2018; Nandiyanto et al., 2019). In this study, FTIR analysis was conducted to characterize the chemical structures of the experimental samples, using a JASCO FT/IR 4700 model spectrometer.

4.9 Brunauer–Emmett–Teller (BET) and Scanning Electron Microscopy (SEM) Analysis

The Brunauer–Emmett–Teller (BET) technique was employed to evaluate the pore size distribution and surface area of powdered or solid samples containing micro-, meso-, and macropores through physical adsorption under varying pressure conditions. BET measurements were carried out using the QUANTACHROME AUTOSORB IQ2 instrument. Additionally, Scanning Electron Microscopy (SEM) analyses were performed in the same laboratory to provide further insight into the morphological characteristics of the samples.

4.10 Adsorption Studies

In this study, MB dye was used as the adsorbate. MB is a dark blue dye that is readily soluble in water and ethanol, and exhibits strong affinity toward aqueous media. The structural formula and key properties of the MB molecule are presented in Table 2 and Fig. 2.

Following MB adsorption, the concentration of unadsorbed MB remaining in the aqueous solution was determined via spectrophotometric analysis using a Merck Spectroquant Pharo300 UV/VIS device. Based on the residual MB concentration, the amount of adsorbate adsorbed per gram of adsorbent and the adsorption efficiency percentage were calculated using the formulas provided in Eqs. (11) and (12), expressed in mg/g.

$$q_e = \frac{(C - C_e x V)}{m} \tag{11}$$

$$Adsorption(\%) = \frac{C - C_e}{C} x100 \tag{12}$$

qe Amount of adsorbate adsorbed per unit mass of adsorbent (mg/g).

C Initial concentration of the adsorbate (mg/L).

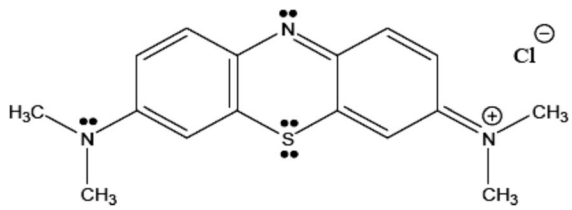


Fig. 2 Structural formula of the MB molecule

Table 2 Properties of the dye used in the study

Sample Name	Chemical Name	CAS Number	Brand Name	Chemical Formula	Color
Methylene Blue	3,7-bis (Dimethylamino)- phenazathionium chloride	122965–43-9	Merck	$C_{16}H_{18}ClN_3S.3H_2O$	Blue

Ce Equilibrium concentration of the adsorbate remaining in solution (mg/L).

V Volume of the solution (L).

m Mass of the adsorbent (g).

In the experiments conducted with MB dye, absorbance measurements were performed at a wavelength of 665 nm. A stock solution of MB with a concentration of 500 mg/L was prepared and subsequently diluted to the required concentrations for use in the adsorption studies.

4.11 Effect of Initial Solution pH on MB Adsorption

The pH values of 20 mg/L MB solutions were adjusted to 4, 5.5, 6, 6.5, 7, and 9 using 0.1 N HCl and 0.1 N NaOH solutions (Merck). Subsequently, 2.5 g/L of activated carbon was added to each solution, and adsorption experiments were carried out under these conditions.

4.12 Effect of Initial Dye Concentration on MB Adsorption

To investigate the effect of initial dye concentration on adsorption performance, MB solutions were prepared at varying concentrations of 0, 15, 20, 25, 30, 40, and 50 mg/L. Each solution was treated with 2.5 g/L of activated carbon, and adsorption experiments were subsequently conducted.

4.13 Effect of Adsorbent Dose on MB Adsorption

Adsorption experiments were continued by adding activated carbon at concentrations of 2.5, 3.75, 5, 7.5, 10, and 15 g/L to solutions with initial MB concentrations of 0, 15, 20, 25, 30, 40, and 50 mg/L. All experiments were conducted at pH 4. During the adsorption studies, samples were collected at 0, 15, 30, 45, 60, 90, and 120 min. The obtained data were analyzed by applying pseudo-first-order and pseudo-second-order kinetic models, and adsorption kinetics were interpreted based on the plotted graphs and calculated parameters.

4.14 Effect of Temperature on MB Adsorption

To evaluate the effect of temperature on dye removal, MB solutions with concentrations of 0, 15, 20, 25, 30, 40, and 50 mg/L were prepared from the stock solution. Adsorption experiments were conducted at temperatures of 283, 293, 303, and 313 °K. An adsorbent dosage of 2.5 g/L was used in all experiments, which were carried out at a fixed pH of 4.

5 Results

The moisture, ash, and solid content values presented in Table 3 confirm the suitability of the SCG samples for the pyrolysis process.

According to the literature, the optimal moisture content for feedstocks intended for thermal conversion processes should range between 5 and 35% (Belgiorno et al., 2003; Demirbas, 2009). The moisture content determined in this study (8.28%) falls within this ideal range, indicating the appropriateness of the SCG samples for pyrolysis. Furthermore, the high solid content (91.72%) provides additional evidence supporting their suitability.

The properties of the feedstock play a critical role in influencing pyrolysis efficiency, with materials rich in carbon and hydrogen being particularly favorable. Consequently, thermal value analyses were performed to assess the feasibility of utilizing SCG for pyrolysis, and the thermal characteristics of both the raw SCG and the resulting biochars are detailed in Table 3.

Table 3 Results of moisture, ash amount, solid matter and burning loss tests and energy values of biochar after pyrolysis and physical activation

Sample	Moisture (%)	Ash amount (%)	Solid matter (%)	Combustion loss (%)	Energy value (cal/g)
Raw SCG	8.28	98.08	91.72	98.08	5121
600℃ pyrolysis product biochar activated at 900℃	3.45	79.25	96.55	79.25	6555

5.1 BET Analysis Results

The evaluation of adsorption capacity is highly dependent on the surface area of the adsorbent material. Key factors influencing surface area and pore structure include the inherent structural properties of the raw material, the activation technique employed, and operational parameters such as activation temperature and duration (Hadi et al., 2015).

Surface area measurements could not be performed on the unactivated pyrolysis products. Therefore, BET analysis was conducted on biochars that were activated at 900 °C in the presence of CO_2 gas following pyrolysis. The activated carbon produced from SCG by pyrolysis at 600 °C followed by physical activation exhibited the highest specific surface area (44.59 m^2/g) among the SCG-derived biochars prepared at different pyrolysis temperatures in this study.

In addition, the material showed a total BET pore volume of 0.028 cm^3/g and an average pore diameter of 2.51 nm, indicating a porous structure dominated by small mesopores, with possible contributions from micropores.

These values are comparable to those reported in the literature for SCG-derived biochars produced under similar thermochemical conditions. For instance, Islam et al. (2024) reported a maximum BET surface area of 40.1 m^2/g for SCG biochar obtained at a pyrolysis temperature of 500 °C, accompanied by a pore volume of 0.019 cm^3/g and an average pore diameter of 3.28 nm (Islam et al., 2024).

Likewise, Alves et al. (2019) reported that biochars derived from coffee residues generally exhibit moderate surface areas and limited pore volumes, with pore structures predominantly within the micro- to mesoporous range (Alves et al., 2019). These comparisons indicate that the BET surface area and pore characteristics obtained in the present study are in good agreement with previously reported SCG-based biochars and reflect typical textural properties of coffee-derived carbon.

5.2 SEM Images

SEM was employed to examine whether the pore structures of the biochars produced through pyrolysis are suitable for adsorption processes. To evaluate the morphological changes induced by pyrolysis and subsequent physical activation, SEM images of the raw material as well as the biochars after treatment stage are presented in Figs. 3 to 4.

The SEM analysis of untreated raw SCG (Fig. 3) reveals a smooth surface morphology lacking visible porosity. However, as the pyrolysis temperature increases and the resulting biochars undergo physical activation, a significant development in pore structure is observed, indicating enhanced porosity in the treated samples (Fig. 4).

5.3 Elemental Analysis Results

Feedstocks with high carbon and hydrogen content are regarded as highly suitable for pyrolysis applications. Accordingly, elemental analysis was initially performed to assess the suitability of SCG samples for pyrolytic conversion. The elemental composition data for both the raw SCG and the biochar derived from it are summarized in Table 4.

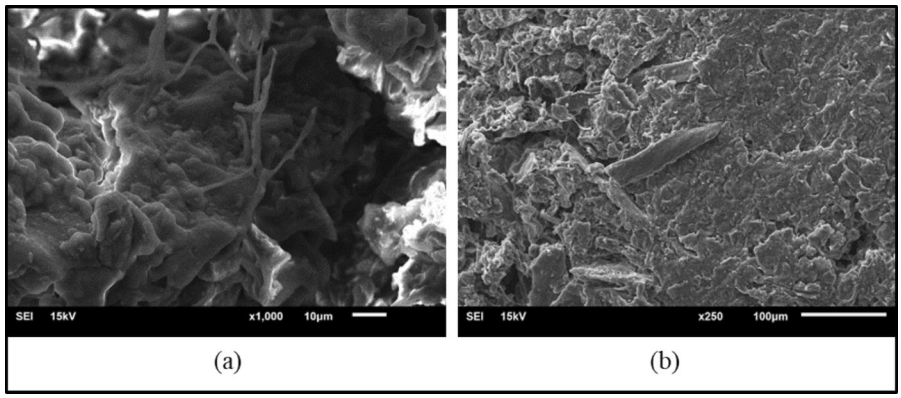


Fig. 3 SEM images of raw SCG. **a**- magnified 1000 times **b**- magnified 250 times

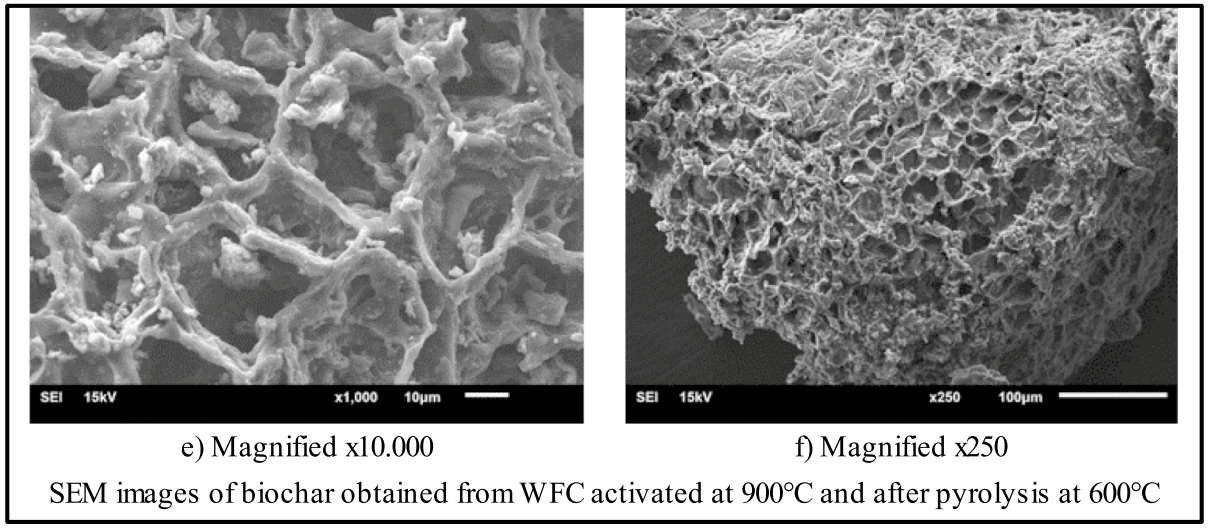


Fig. 4 SEM images of biochar obtained from SCG activated at 900 °C and after pyrolysis at 600 °C

Table 4 Elemental Analysis Results

Sample	C%	H%	N%
SCG	50.84	6.87	2.295
Biochar obtained by pyrolysis at 600℃, activated at 900℃	81.53	2.48	1.05

Elemental analysis revealed that the raw SCG sample contains 85.35% carbon and 7.70% hydrogen. These high values confirm the suitability of SCG as a potential feedstock for pyrolysis processes, consistent with findings reported in the literature (Tsai et al., 2012).

5.4 FTIR Analysis Results

SCG typically contains approximately 1–2% caffeine. In the FTIR spectrum shown in Fig. 5, the stretching vibrations at 2923 cm^{-1} and 2854 cm^{-1} are attributed to the presence of caffeine. Chlorogenic acids, which make up roughly 5–10% of coffee content, exhibit characteristic absorption bands at 1704 cm^{-1} and 1635 cm^{-1} due to their ester functional groups. Furthermore, the C–N stretching vibration associated with tertiary amines found in caffeine, theobromine, and theophylline molecules generally appears within the 1350–1200 cm^{-1} range, and is detected at 1247 cm^{-1} in this study. Depending on storage conditions, coffee also contains approximately 2–5% moisture, and the stretching vibration band of water molecules is observed at 3294 cm^{-1} in the FTIR spectra (Barrios-Rodríguez et al., 2021).

Following high-temperature pyrolysis of coffee, the thermal degradation of its organic constituents leads to the formation of char and low-molecular-weight compounds. The disappearance of multiple absorption bands in the FTIR spectra, as shown in Fig. 6, provides clear evidence of this decomposition. The resulting char primarily comprises amorphous carbon and graphite-like structures. The absorption bands observed between 3000 cm^{-1} and 2900 cm^{-1} correspond to C–H stretching vibrations associated with residual hydrocarbon groups. Additionally, the bands in the 1600–1500 cm^{-1} range are attributed to C = C stretching vibrations originating from aromatic structures.

5.5 Adsorption Studies

In this study, the adsorption of MB dye onto activated carbon derived from SCG was investigated. The experiments were conducted in a batch system under constant stirring conditions, with variations in temperature and dye concentration.

The adsorption studies examined the effects of initial pH, temperature, initial MB concentration, and varying adsorbent dosages on MB removal efficiency. The experimental data obtained were fitted to

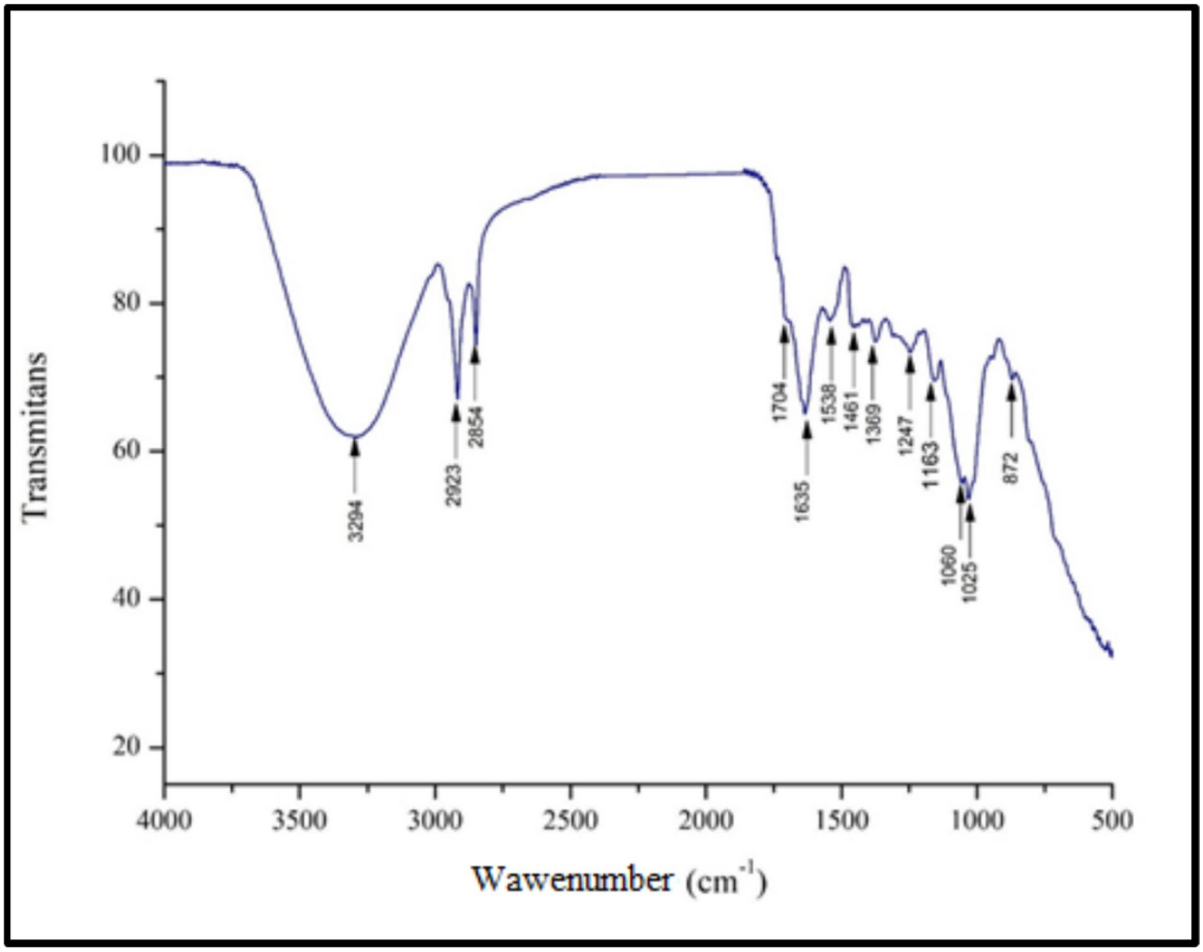


Fig. 5 FTIR Spectra of SCG

Langmuir, Freundlich, and Temkin isotherm models for comparative evaluation. Additionally, pseudo-first-order and pseudo-second-order kinetic models were applied to the data to determine the adsorption rate expressions.

5.5.1 Effect of Initial pH on MB Adsorption

In this study, the effect of varying pH levels on MB adsorption was investigated, and the relationship between removal efficiency and contact time was thoroughly evaluated. The point of zero charge (pHpzc) of the activated carbon derived from SCG was determined using the pH drift method and found to be approximately 6.4. This value indicates that the surface of the adsorbent is positively charged below pH 6.4 and negatively charged above it. At pH 4, which is below the pHpzc, the electrostatic attraction between the protonated surface and the cationic MB molecules is relatively weak; however, adsorption can still occur through π–π stacking and van der Waals interactions between the aromatic structures of MB and the carbon matrix. As the pH increases beyond the pHpzc, the surface becomes negatively charged due to deprotonation, resulting in electrostatic repulsion and reduced adsorption efficiency. These findings align with previous reports on coffee husk–derived activated carbons, where pHpzc values of 6.94 and 6.63 were obtained for KOH- and H_3PO_4-activated samples, respectively (Ngueabouo et al., 2022).

The variation in adsorption efficiency with pH can be further explained by the protonation–deprotonation behavior of surface functional groups such as

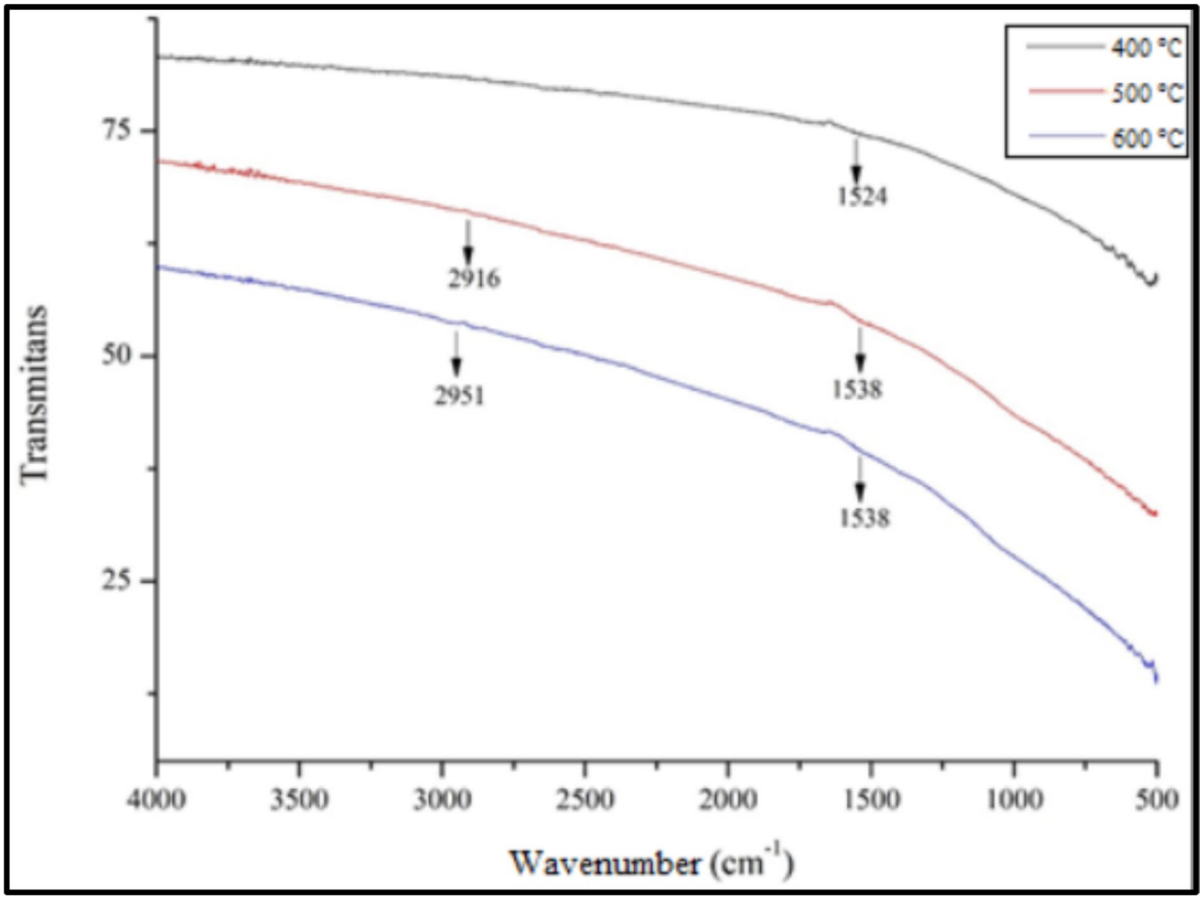


Fig. 6 FTIR Spectra of biochar obtained as a result of pyrolysis of coffee at different temperatures and activation at 900℃

hydroxyl and carboxyl moieties (Qiu et al., 2022). Below the pHpzc, surface hydroxyl and carboxyl groups are predominantly protonated, decreasing the availability of negatively charged adsorption sites and limiting electrostatic attraction with cationic MB molecules. In this acidic regime, non-electrostatic interactions primarily π–π stacking and van der Waals forces play a major role in dye adsorption. Conversely, at pH values above the pHpzc, surface deprotonation increases the negative charge density, leading to stronger electrostatic repulsion and a decline in overall adsorption capacity.

The results demonstrated that under acidic conditions (pH 4), adsorption occurred both rapidly and effectively, achieving a removal efficiency of 98.99% within the first 15 min, which remained nearly constant in subsequent time intervals (Fig. 7). This behavior suggests that the positively charged adsorbent surface and the aromatic nature of the carbon facilitate strong MB adsorption through multiple interaction mechanisms. As the pH increased particularly at pH 7 and 9 a gradual decline in removal efficiency was observed over time. At pH 9, the removal rate decreased from 95.26% at 15 min to 90.54% at 120 min. This reduction can be attributed to the increased competition from OH^- ions at higher pH values and the shift in surface charge toward negativity, which collectively hinder dye binding. In summary, optimal adsorption performance was achieved under acidic conditions, while increasing pH resulted in a gradual decrease in efficiency.

Additionally, in a study conducted by Hayu et al. (2022), the adsorption of MB onto activated carbon derived from durian peel was investigated. Within the pH range of 2 to 5, both the removal efficiency and adsorption capacity of MB increased significantly.

This enhancement was attributed to the reduction of negative surface charge at lower pH values, which led to stronger electrostatic attraction between the positively charged MB molecules and the adsorbent surface (Hayu et al., 2022).

Variations in solution pH can lead to structural changes in the adsorbate molecules. As shown by the data in Fig. 7, the observed changes in removal efficiency with respect to pH justified the selection of pH 4 for subsequent experiments. The adsorption of MB from aqueous solutions is generally recognized as a pH-sensitive process. Many studies have reported that cationic dyes such as MB are more effectively adsorbed in the pH range of 6 to 11, as surface charges in this range are more favorable for attracting dye molecules. However, the optimal pH range can vary depending on the properties of the adsorbent. For instance, the ideal pH range may differ when using adsorbents such as activated carbon or natural clays.

Cationic dyes such as MB can remain stable under acidic conditions, including at pH 4; however, several studies have reported that adsorption capacity tends to improve at higher pH levels. At low pH, the molecular structure of MB is not expected to degrade, although the efficiency of the adsorption process may be reduced. Since the likelihood of dye molecule degradation under acidic conditions is minimal, the observed color removal can be attributed primarily to actual dye adsorption rather than chemical decomposition (El-Halwany, 2010; Hameed et al., 2007; Wang et al., 2005).

5.5.2 *Effect of Adsorbent Dosage on MB Adsorption*

To evaluate the effect of adsorbent dosage on adsorption performance, experiments were conducted using varying amounts of activated carbon in the range of 2.5 to 15 g/L under constant conditions of pH 4 and 293 K. The time-dependent MB removal efficiencies

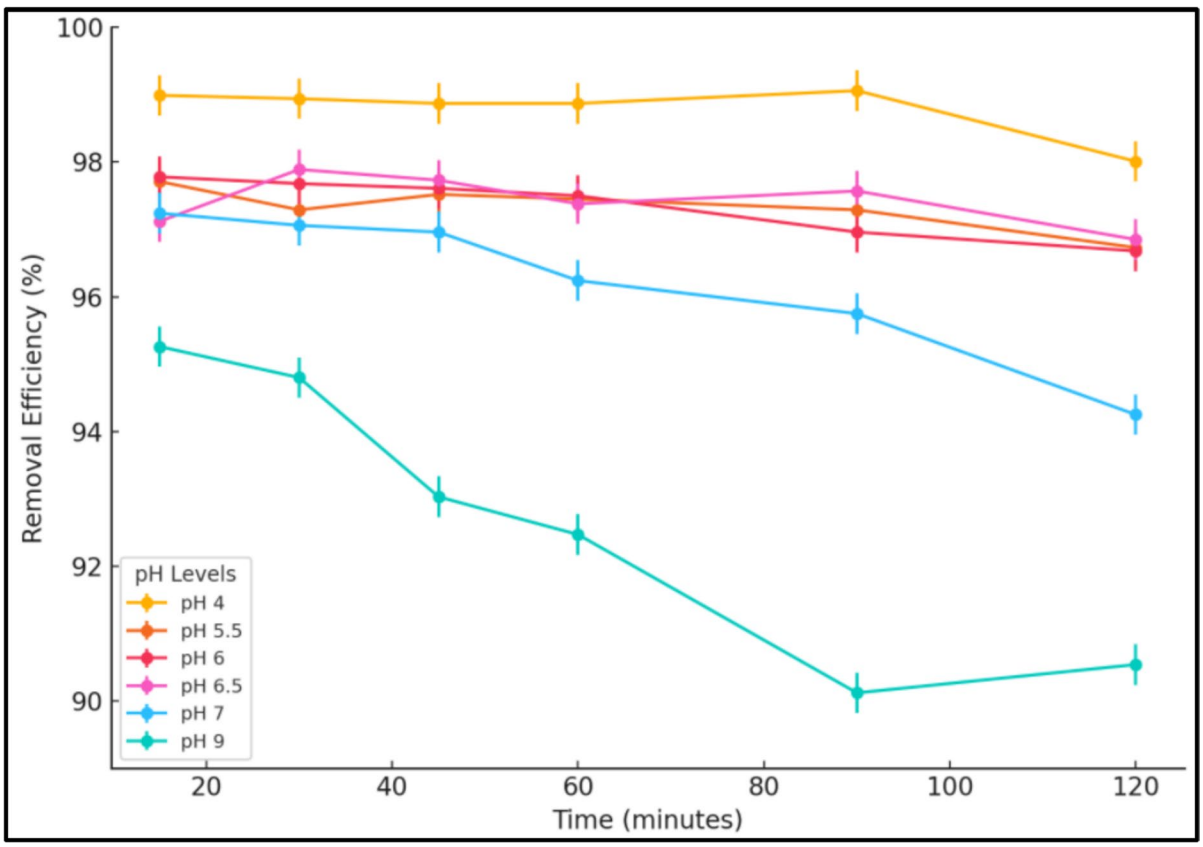


Fig. 7 Variation of MB removal over time at different pH levels (T = 293 K, C_0 = 20 mg/L, stirring speed = 200 rpm)

for different adsorbent doses are presented in Fig. 8. The results demonstrate that the activated carbon produced from pyrolyzed SCG exhibits remarkably high adsorption efficiency. Across all tested dosages (2.5–15 g/L) and contact times (15–120 min), MB removal ranged between 98.78% and 99.15%, with equilibrium being reached within the first 15 min. Notably, even at the lowest dosage of 2.5 g/L, a removal efficiency of 99.08% was achieved, confirming the material's strong adsorption capacity and cost-effectiveness.

The marginal increase in removal efficiency with higher adsorbent dosage indicates that most active sites were already saturated at lower concentrations, suggesting the presence of highly accessible and energetically favorable adsorption sites. The rapid equilibrium attainment further reflects strong surface affinity between MB molecules and the SCG-derived activated carbon. These characteristics highlight the material's potential as a fast, efficient, and sustainable adsorbent for dye removal applications.

5.5.3 *Effect of Initial Concentration on MB Adsorption*

The dye removal efficiencies obtained under optimal experimental conditions are presented in Fig. 9. Upon examining the results with respect to variations in the initial dye concentration, it was observed that the highest removal efficiency was achieved at an initial concentration of 20 mg/L. Considering all initial concentrations, the removal efficiencies were found to range between 66.00% and 99.95% (Fig. 9).

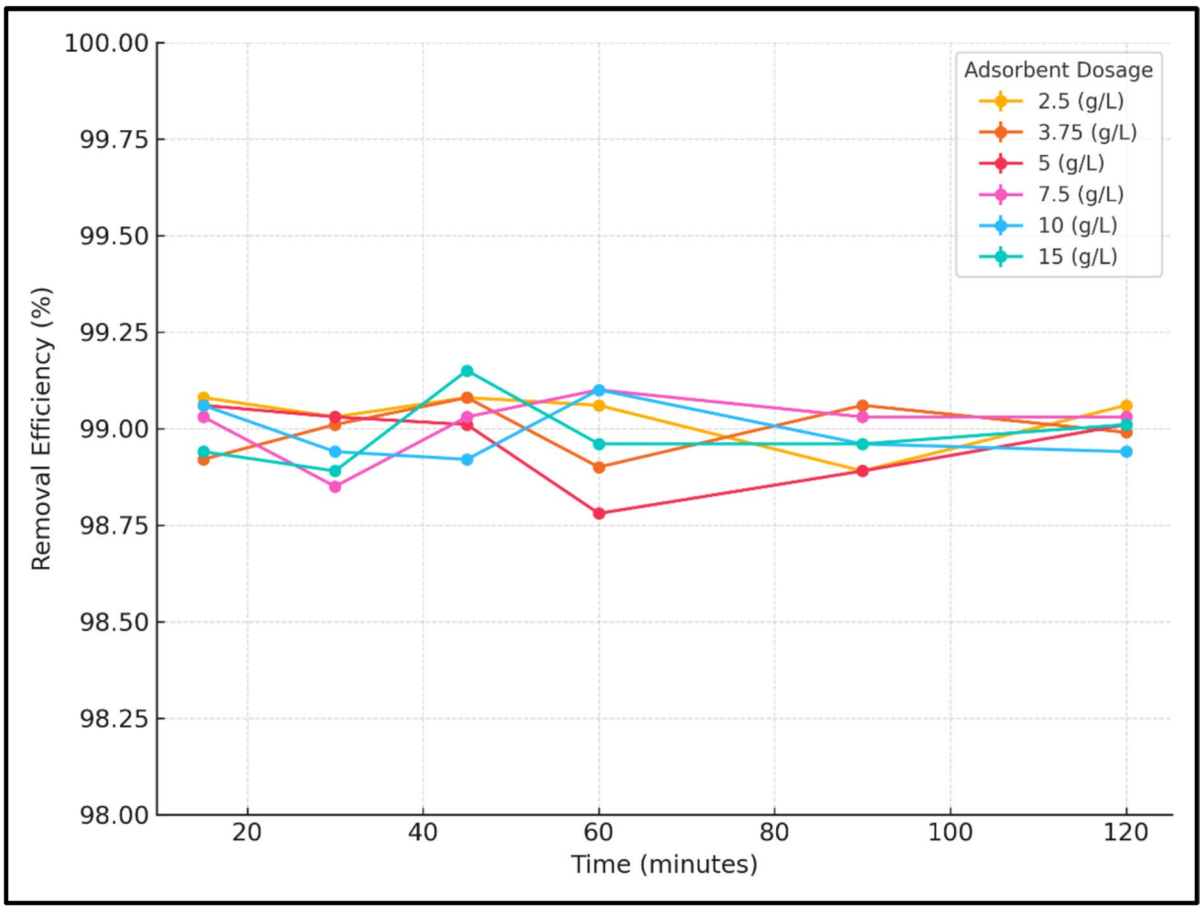


Fig. 8 Variation of MB removal over time for different adsorbent dosages (T = 293 K, C_0 = 20 mg/L, stirring speed = 200 rpm)

The observed removal efficiency trend rapid dye adsorption in the first 30–45 min followed by a plateau is highly consistent with recent studies utilizing activated carbon derived from SCG. These studies show that adsorption kinetics typically follow a pseudo-second-order model, suggesting that surface-related interactions, possibly involving chemisorption, may control the rate-limiting step, with equilibrium reached around 40–60 min (Aouay et al., 2024). For instance, Chiang et al. (2020) reported extremely high dye adsorption capacities with equilibrium behavior best described by the Langmuir isotherm model (Chiang et al., 2020).

Furthermore, adsorption studies with spent coffee ground biochar show that the removal percentage increases with time but levels off due to site saturation similar to the plateau seen in your results (Adamu et al., 2023). These findings confirm that the adsorption behavior captured in your graph is typical of biomass-derived activated carbon systems and align with kinetic and equilibrium modeling observed in the literature (Chen et al., 2022).

5.5.4 Effect of Temperature on MB Adsorption

To assess the effect of temperature on adsorption performance, experiments were conducted across a temperature range of 283–313 K using adsorbent dosages between 2.5 and 15 g/L at pH 4, with an initial MB concentration of 20 mg/L. The time-dependent MB removal efficiencies at different temperatures are presented in Fig. 10.

MB adsorption experiments clearly demonstrated that temperature influences both adsorption kinetics and overall efficiency. At 283 K, the removal efficiency reached 73% within the first 15 min, whereas this value increased to 90% at 293 K, indicating that elevated temperatures enhance molecular mobility and surface interactions, thereby accelerating the adsorption process. At 293 K, a maximum efficiency of 91% was maintained throughout the process. At higher temperatures (303–313 K), removal efficiencies of 88–90% were also obtained, suggesting that temperature primarily affects the adsorption rate rather than the final capacity. The relatively low initial efficiency observed at 303 K (65% in the first 15 min)

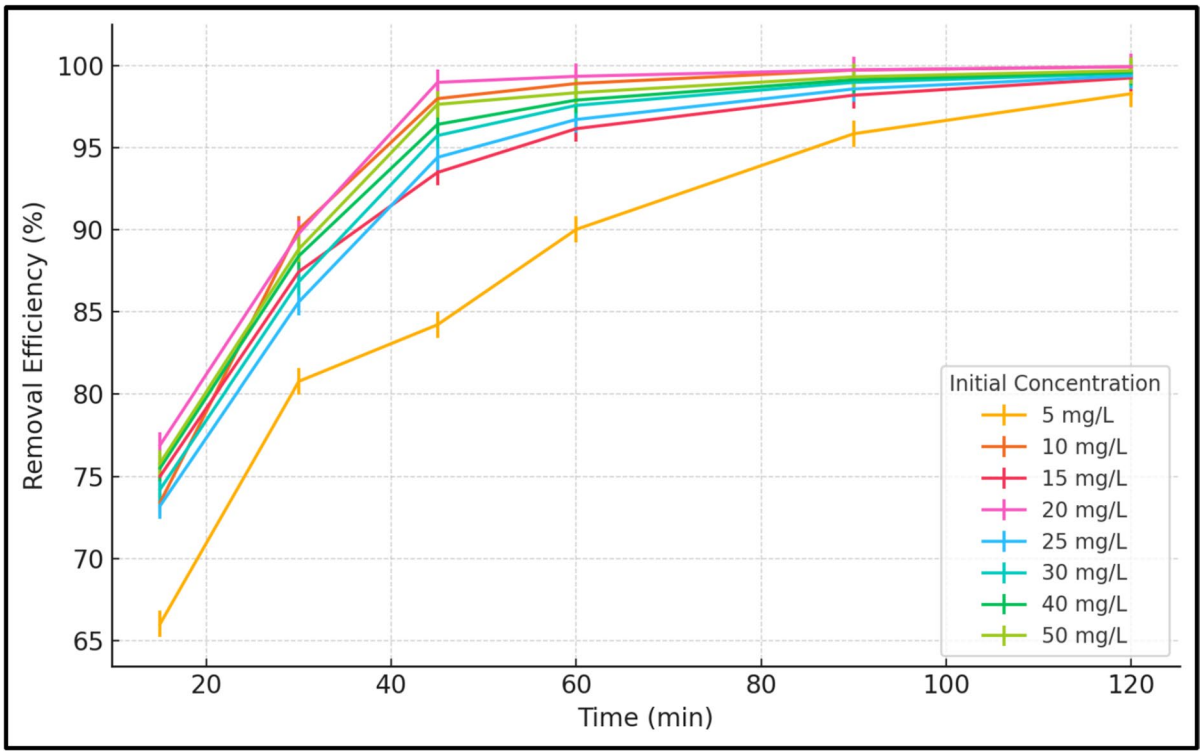


Fig. 9 MB Removal Efficiencies (T = 293 K, stirring speed = 200 rpm, 2.5 gr adsorban/L, pH = 4)

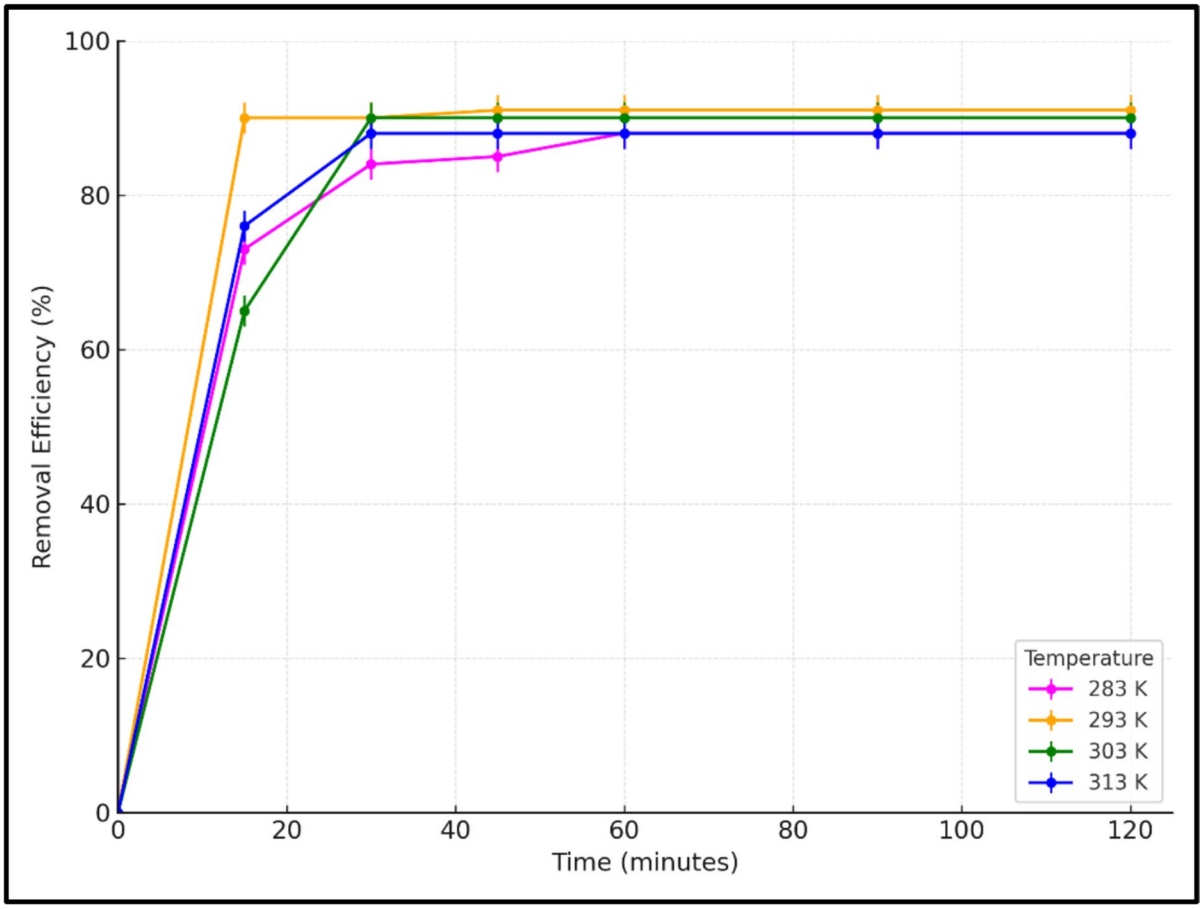


Fig. 10 Time-dependent variation of MB removal at different temperatures

may indicate a transient kinetic delay before equilibrium is reached. Overall, 293 K emerged as the most favorable temperature for rapid and stable adsorption under the experimental conditions.

The observed improvement in adsorption efficiency at elevated temperatures suggests that the process is endothermic. Increased temperature enhances molecular diffusion and facilitates the penetration of MB molecules into the internal pores of the adsorbent, which may be related to surface interactions, potentially involving electron exchange between the dye molecules and surface functional groups. These findings are consistent with previous studies reporting optimal MB adsorption within the 303–323 K range (Marrakchi et al., 2017; Tan et al., 2008). In general, moderate to slightly elevated temperatures enhance adsorption efficiency, suggesting that endothermic activation plays a significant role in dye removal performance.

5.5.5 Isotherm Studies

The Freundlich and Temkin isotherm constants are presented in Table 5.

As shown in Table 5, the adsorption mechanism of MB fits the Freundlich isotherm model with a correlation coefficient (R^2) of 0.9924. For the Temkin isotherm, the R^2 value was determined to be 0.8693, while for the Langmuir isotherm, the R^2 value was found to be 0.0985. The extremely poor fit of the Langmuir isotherm indicates that the adsorption of MB onto the SCG-derived activated carbon does not follow monolayer adsorption on a homogeneous surface with energetically identical sites. This behavior can be attributed to the heterogeneous surface structure of the physically activated carbon, which contains a wide distribution of adsorption sites with

Table 5 Freundlich and Temkin Isotherm Constants

K_f (mg/g)	n	1/n	R^2	KT (L/g)	B (J/mol)	R^2
8.412	1.035	0.966	0.9924	1.026	386.39	0.8693

different energies due to the coexistence of micro- and mesopores and surface functional groups.

In the Freundlich isotherm, the value of 1/n represents the heterogeneity factor and typically falls within the range of 0 to 1. The closer the 1/n value is to zero, the more heterogeneous the surface is considered to be. An "n" value greater than 1 indicates that the adsorption process is favorable and that physical adsorption mechanisms are predominant. Conversely, if the "n" value is less than 1, it suggests that chemical adsorption processes are dominant. The constant K_f in the Freundlich isotherm represents the adsorption capacity of the adsorbent (Na, 2020; Okpara et al., 2021).

For this study, the "n" value obtained from the Freundlich isotherm was determined to be 1.035, indicating that physical adsorption is more dominant than chemical adsorption. This result suggests the presence of weak adsorption forces, such as Van der Waals interactions (Ofomaja, 2008). However, this interpretation does not contradict the pseudo-second-order kinetic model, which suggests that surface-related interactions, possibly involving chemisorption, may be associated with the rate-limiting step. The Freundlich 'n' value (1.035), being close to unity, supports the possible coexistence of physical and chemical adsorption processes, indicating a borderline or mixed adsorption behavior. In heterogeneous adsorption systems, including SCG-derived activated carbons, multiple interaction mechanisms may coexist. The kinetic behavior suggests that chemisorption-related processes may influence the adsorption rate, while the Freundlich isotherm implies that multilayer physisorption may contribute to the equilibrium stage. Therefore, the overall adsorption process can be described as a mixed adsorption mechanism. Accordingly, the kinetic and equilibrium analyses are complementary rather than contradictory, jointly indicating a mixed adsorption mechanism.

In the Temkin isotherm, KT represents the binding energy at equilibrium, while B is a parameter related to the heat of adsorption. Upon examining the data presented in Table 5, it is observed that the R^2 value for the Temkin isotherm ($R^2 = 0.8693$) is lower than that of the Freundlich isotherm but higher than that of the Langmuir isotherm. Therefore, the Freundlich isotherm more accurately represents the adsorption behavior. In the study conducted by Özbaş et al. (2019), it was reported that the adsorption of MB using biochar activated with $ZnCl_2$ after the pyrolysis of waste tires could be described by the Freundlich isotherm. In the study by Ciner et al. (2024a), nickel removal by adsorption from a synthetically prepared nickel solution using biochars obtained through carbonization was investigated. It was determined that the adsorption of nickel with SCG-derived biochar could be best represented by the Langmuir isotherm.

The superior fit to the Freundlich model indicates multilayer adsorption on a heterogeneous surface, which is consistent with the coexistence of micro- and mesopores observed in SEM and BET analyses. The heterogeneity of the surface enhances the adsorption of MB through both physical and chemical interactions across sites of varying energy.

5.5.6 Kinetic Calculations

In the MB adsorption study, pseudo-first-order and pseudo-second-order kinetic models were examined to analyze the adsorption mechanism, and the corresponding kinetic constants were calculated for each model.

Calculations based on the pseudo-first-order model revealed relatively low correlation coefficients (R^2 values ranging from 0.06 to 0.81), indicating that MB adsorption using activated carbon derived from SCG could not be adequately described by this model. In contrast, the kinetic parameters obtained from the pseudo-second-order model are presented in Table 6.

The correlation coefficient (R^2) values calculated for the pseudo-second-order kinetic model were found to range between 0.94 and 1.00 (Table 6). These results indicate that the pseudo-second-order model provides a good fit for describing the adsorption of MB using activated carbon derived from SCG.

Table 6 Kinetic constants

Co (mg/L)	pH	Adsorban miktarı (g/L)	R^2	k_2 (g min/mg)	qe experimental (mg/g)	qe calculation (mg/g)
20	4	2.5	0.9731	1.822	0.16	0.108
20	5.5	2.5	0.971	0.588	0.262	0.252
20	6	2.5	0.9664	0.357	0.266	0.269
20	6.5	2.5	0.9529	0.610	0.253	0.238
20	7	2.5	0.9438	0.165	1.26	0.403
20	9	2.5	0.885	0.058	0.96	0.904
20	4	3.75	1	4.484	7.93	5.279
20	4	5	1	25.523	7.93	3.959
20	4	7.5	1	24.295	7.93	2.641
20	4	10	1	220.75	7.93	1.320
20	4	15	1	220.75	7.93	1.320

A review of the literature shows that the kinetic results obtained in this study are consistent with those reported in similar studies on dye removal from liquid phases. Kinetic studies on dye adsorption have generally shown that the pseudo-second-order kinetic model is suitable for describing the adsorption behavior (Gündoğdu, 2010; Ofomaja, 2008; Ongen et al., 2012; Özbaş et al., 2019).

Based on the evaluation of the obtained data, the pseudo-second-order kinetic model was found to be the most appropriate for describing the adsorption process. This outcome may vary depending on the chemical structure of the material under different physicochemical experimental conditions such as pH, dye concentration, adsorbent dosage, and temperature. The results suggest that surface-related interactions, possibly involving chemisorption, may contribute to the rate-limiting step of the adsorption process.

The good fit of the pseudo-second-order model suggests that surface-related interactions, potentially involving chemisorption through electron exchange between MB molecules and active surface sites, may influence the adsorption rate. The initial rapid uptake phase can be attributed to the availability of abundant surface sites, whereas the subsequent stage may be governed by intraparticle diffusion.

5.5.7 Adsorption Thermodynamics

To further understand the mechanism of adsorption, thermodynamic parameters were evaluated based on equilibrium data at different temperatures (Table 7). The positive enthalpy change ($\Delta H^\circ = +21.48$ kJ/mol) indicated that the adsorption process was endothermic, suggesting that higher temperatures favor dye removal. Additionally, the positive entropy change ($\Delta S^\circ = +85.58$ J/mol·K) implied an increase in randomness at the solid–liquid interface during adsorption, possibly due to desorption of water molecules and rearrangement of dye molecules on the adsorbent surface. The Gibbs free energy change (ΔG°) values were calculated as –2.71, –3.79, –4.12, and –5.46 kJ/mol at 283, 293, 303, and 313 K, respectively. The negative values of ΔG° confirmed the spontaneous nature of the process, and the increasing spontaneity with temperature further supported the endothermic character of the adsorption.

Table 7 Thermodynamic parameter values

Temperature (K)	Ln (Kc)	ΔG° (kJ/mol)
283	1.1524	–2.7115
293	1.5554	–3.7889
303	1.6372	–4.1243
313	2.0993	–5.4629

The environmental and economic advantages of producing physically activated carbon from SCG are both substantial and multidimensional. Environmentally, the utilization of SCG as a carbon precursor mitigates the environmental burden associated with landfill disposal and the consequent emission of methane, a potent greenhouse gas. Furthermore, employing CO_2 as the activating agent promotes its valorization, transforming a greenhouse gas into a functional process medium. Unlike conventional chemical

activation methods that typically involve corrosive reagents such as $ZnCl_2$ or H_3PO_4, CO_2-based physical activation generates no acidic or saline effluents, thereby significantly reducing the risk of secondary pollution and post-treatment requirements (Chew et al., 2023; Heidarinejad et al., 2020).

From an economic standpoint, SCG represents an almost cost-free, readily available feedstock derived from the food and beverage industry. The elimination of costly chemical activating agents and the reduced need for wastewater treatment collectively help lower overall production costs compared with conventional chemical activation methods (León et al., 2020). Although the process requires relatively high activation temperatures (around 900 °C), the associated energy costs can be mitigated through energy recovery strategies or the integration of renewable energy sources, thereby maintaining the economic feasibility of large-scale implementation.

6 Conclusions

This study systematically evaluated the production and adsorption performance of physically activated carbon derived from SCG through controlled pyrolysis followed by CO_2-assisted activation. The results confirm that SCG is a suitable and versatile precursor for the synthesis of functional carbon materials with adsorption capability toward MB.

Among the prepared samples, the biochar obtained via pyrolysis at 600 °C and subsequent activation at 900 °C exhibited the most favorable textural properties. This material achieved a BET surface area of 44.59 m^2/g, a total pore volume of 0.028 cm^3/g, and an average pore diameter of 2.51 nm, indicating a porous structure dominated by small mesopores, with possible contributions from micropores. These textural properties are consistent with previously reported non-chemically activated SCG-derived biochars produced under similar thermochemical conditions and confirm that the obtained surface area falls within the typical range reported for such materials.

Batch adsorption experiments demonstrated high MB removal efficiencies, reaching up to 99.15% under optimized conditions, with rapid adsorption kinetics and equilibrium attained within short contact times. Kinetic modeling indicated that the adsorption process followed the pseudo-second-order model, suggesting that surface-related interactions, potentially involving chemisorption, may be associated with the adsorption rate. Equilibrium data were best described by the Freundlich isotherm, reflecting multilayer adsorption on a heterogeneous surface. The limited applicability of the Langmuir model further implies that MB adsorption may not occur through ideal monolayer coverage on energetically uniform sites.

Overall, the results demonstrate that surface chemistry and pore accessibility play a more decisive role than surface area alone in governing the adsorption performance of SCG-derived physically activated carbons. Despite exhibiting a moderate BET surface area compared with CACs, the presence of accessible micro–mesopores and surface functional groups enables highly efficient dye removal, highlighting the importance of textural quality and surface heterogeneity over surface area magnitude.

From a sustainability perspective, the use of SCG as a carbon precursor and CO_2 as a physical activating agent offers clear environmental advantages by avoiding corrosive chemicals and reducing secondary pollution. While the high adsorption efficiency and low-cost feedstock suggest promising practical potential, a detailed techno-economic assessment and life-cycle analysis were beyond the scope of this study and should be addressed in future work.

Future studies should focus on adsorbent regeneration and reuse, adsorption–desorption cyclic stability, and performance evaluation under continuous-flow or column conditions. In addition, quantitative assessments of economic feasibility and environmental impacts will be essential to further validate the large-scale applicability of SCG-derived physically activated carbons for wastewater treatment applications.

Author Contribution Conceptualization, M.N.C., E.E.Ö. and H.K.Ö.; methodology, M.N.C., E.E.Ö., H.K.Ö. and A.Ö.; investigation, M.N.C., E.E.Ö. and H.K.Ö.; writing—original draft preparation, M.N.C., E.E.Ö., H.K.Ö. and A.Ö. All authors have read and agreed to the published version of the manuscript.

Funding Open access funding provided by the Scientific and Technological Research Council of Türkiye (TÜBİTAK).

Data Availability All data related to the study are provided within the paper.

Declarations

Ethics Approval Not applicable.

Consent for Publication The paper is submitted with the consent of all authors.

Competing Interests The authors declare no competing interests.

Open Access This article is licensed under a Creative Commons Attribution 4.0 International License, which permits use, sharing, adaptation, distribution and reproduction in any medium or format, as long as you give appropriate credit to the original author(s) and the source, provide a link to the Creative Commons licence, and indicate if changes were made. The images or other third party material in this article are included in the article's Creative Commons licence, unless indicated otherwise in a credit line to the material. If material is not included in the article's Creative Commons licence and your intended use is not permitted by statutory regulation or exceeds the permitted use, you will need to obtain permission directly from the copyright holder. To view a copy of this licence, visit http://creativecommons.org/licenses/by/4.0/.

References

Adamu, A., Zewge, F., & Chebude, Y. (2023). Adsorption activity of spent coffee grounds biochar for the removal of vivizole red 3BS dye from aqueous solution. *International Journal of Environmental Research, 17*(4), Article 46.

Ahmad, A., Mohd-Setapar, S. H., Chuong, C. S., Khatoon, A., Wani, W. A., Kumar, R., & Rafatullah, M. (2015). Recent advances in new generation dye removal technologies: Novel search for approaches to reprocess wastewater. *RSC Advances, 5*(39), 30801–30818.

Ahmed, H., Abolore, R. S., Jaiswal, S., & Jaiswal, A. K. (2024). Toward circular economy: Potentials of spent coffee grounds in bioproducts and chemical production. *Biomass, 4*(2), 286–312.

Akkaya Sayğılı, G., Sayğılı, H., Yılmaz, C., & Güzel, F. (2020). Lead recovery from aqueous environment by using porous carbon of citrus fruits waste: Equilibrium, kinetics and thermodynamic studies. *Separation Science and Technology, 55*(15), 2699–2712.

Al Balushi, J., Al Saadi, S., Ahanchi, M., Al Attar, M., Jafary, T., Al Hinai, M., & Basha, J. S. (2025). A comprehensive review on sustainable conversion of spent coffee grounds into energy resources and environmental applications. *Biomass, 5*(3), Article 55.

Alves, A. C. F., Antero, R. V. P., de Oliveira, S. B., Ojala, S. A., & Scalize, P. S. (2019). Activated carbon produced from waste coffee grounds for an effective removal of bisphenol-A in aqueous medium. *Environmental Science and Pollution Research, 26*(24), 24850–24862.

Aouay, F., Attia, A., Dammak, L., Ben Amar, R., & Deratani, A. (2024). Activated carbon prepared from waste coffee grounds: Characterization and adsorption properties of dyes. *Materials, 17*(13), Article 3078.

Araya-Sibaja, A. M., Quesada-Soto, T., Vega-Baudrit, J. R., Navarro-Hoyos, M., Valverde-Cerdas, J., & Romero-Esquivel, L. G. (2025). Spent coffee ground-based materials evaluated by methylene blue removal. *Processes, 13*(5), Article 1592.

Azargohar, R., & Dalai, A. K. (2008). Steam and KOH activation of biochar: Experimental and modeling studies. *Microporous and Mesoporous Materials, 110*(2–3), 413–421.

Bansal, R. C., & Goyal, M. (2005). *Activated carbon adsorption*. CRC press.

Barrios-Rodríguez, Y., Collazos-Escobar, G. A., & Gutiérrez-Guzmán, N. (2021). ATR-FTIR for characterizing and differentiating dried and ground coffee cherry pulp of different varieties (*Coffea arabica* L.). *Engenharia Agrícola, 41*, 70–77.

Belgiorno, V., De Feo, G., Della Rocca, C., & Napoli, R. M. A. (2003). Energy from gasification of solid wastes. *Waste Management, 23*(1), 1–15.

Campos-Vega, R., Loarca-Pina, G., Vergara-Castañeda, H. A., & Oomah, B. D. (2015). Spent coffee grounds: A review on current research and future prospects. *Trends in Food Science & Technology, 45*(1), 24–36.

Chen, H. M., Lau, W. M., & Zhou, D. (2022). Waste-coffee-derived activated carbon as efficient adsorbent for water treatment. *Materials, 15*(23), Article 8684.

Chew, T. W., H'Ng, P. S., Luqman Chuah Abdullah, B. C. T. G., Chin, K. L., Lee, C. L., Mohd Nor Hafizuddin, B. M. S., & TaungMai, L. (2023). A review of bio-based activated carbon properties produced from different activating chemicals during chemicals activation process on biomass and its potential for Malaysia. *Materials, 16*(23), Article 7365.

Chiang, C. H., Chen, J., & Lin, J. H. (2020). Preparation of pore-size tunable activated carbon derived from waste coffee grounds for high adsorption capacities of organic dyes. *Journal of Environmental Chemical Engineering, 8*(4), Article 103929.

Ciner, M. N., Elmaslar Özbaş, E., Ozcan, H. K., Ongen, A., Eyüboğlu, P., & Cengizoğlu, Z. (2024). Use of biochar obtained from pyrolysis of waste filter coffee as adsorbent for nickel removal. *Chemistry Africa*. https://doi.org/10.1007/s42250-024-01107-w

Ciner, M. N., Özbaş, E. E., Savuk, H., Günay, Ş, Özcan, H. K., & Öngen, A. (2024). The effect of biochar obtained from waste filter coffee grounds on plant germination. *International Journal of Agriculture Environment and Food Sciences, 8*(3), 561–570.

de Bomfim, A. S. C., de Oliveira, D. M., Walling, E., Babin, A., Hersant, G., Vaneeckhaute, C., Dumont, M.-J., & Rodrigue, D. (2022). Spent coffee grounds characterization and reuse in composting and soil amendment. *In Waste, 1*(1), 2–20.

Demirbas, A. (2009). Pyrolysis mechanisms of biomass materials. *Energy Sources, Part A433A: Recovery, Utilization, and Environmental Effects+A465, 31*(13), 1186–1193.

Deribe, H. (2019). Review on factors which affect coffee (*Coffea arabica* L.) quality in South Western, Ethiopia.

International Journal of Forestry and Horticulture, 5(1), 12–19.

El-Halwany, M. M. (2010). Study of adsorption isotherms and kinetic models for Methylene Blue adsorption on activated carbon developed from Egyptian rice hull (part II). *Desalination, 250*(1), 208–213.

Esquivel, P., & Jiménez, V. M. (2012). Functional properties of coffee and coffee by-products. *Food Research International, 46*(2), 488–495.

Gündoğdu, A. (2010). *Fabrika çay atıklarından aktif karbon üretimi, karakterizasyonu ve adsorpsiyon özelliklerinin incelenmesi (in Turkish)* (Doctoral dissertation, Karadeniz Technical University, Institute of Science and Technology). Dissertation No: 270654. https://tez.yok.gov.tr/UlusalTezMerkezi/tezSorguSonucYeni.jsp

Guo, X., & Wang, J. (2019). Comparison of linearization methods for modeling the Langmuir adsorption isotherm. *Journal of Molecular Liquids, 296*, Article 111850.

Güzel, F., Sayğılı, G. A., Sayğılı, H., Koyuncu, F., Kaya, N., & Güzel, S. (2021). Performance of grape (*Vitis vinifera* L.) industrial processing solid waste–derived nanoporous carbon in copper (II) removal. *Biomass Conversion and Biorefinery, 11*(4), 1363–1373.

Hadi, P., Yeung, K. Y., Barford, J., An, K. J., & McKay, G. (2015). Significance of "effective" surface area of activated carbons on elucidating the adsorption mechanism of large dye molecules. *Journal of Environmental Chemical Engineering, 3*(2), 1029–1037.

Hameed, B. H., Din, A. M., & Ahmad, A. L. (2007). Adsorption of methylene blue onto bamboo-based activated carbon: Kinetics and equilibrium studies. *Journal of Hazardous Materials, 141*(3), 819–825.

Hayu, L. D. R., Nasra, E., Azhar, M., & Etika, S. B. (2022). Adsorpsi Zat Warna Methylene Blue Menggunakan Karbon Aktif dari Kulit Durian (Durio zibethinus Murr.). *Jurnal Periodic Jurusan Kimia UNP, 11*(1), 8–13.

Heidarinejad, Z., Dehghani, M. H., Heidari, M., Javedan, G., Ali, I., & Sillanpää, M. (2020). Methods for preparation and activation of activated carbon: A review. *Environmental Chemistry Letters, 18*(2), 393–415.

Ho, Y. S. (2016). Comments on using of "pseudo-first-order model"[J. Taiwan Inst. Chem. Eng. Vol. 59]. *Journal of the Taiwan Institute of Chemical Engineers, 68*, 136–137.

Hsi, H. C., Horng, R. S., Pan, T. A., & Lee, S. K. (2011). Preparation of activated carbons from raw and biotreated agricultural residues for removal of volatile organic compounds. *Journal of the Air & Waste Management Association, 61*(5), 543–551.

International Cofee Organization (ICO), World Cofee Consumption Report (2018). https://en.b2press.com/press-release/1615/cofee-consumption-in-turkey-reached-approximately100-thousand-tons , Accessed 25 May 2024

Ioannidou, O., & Zabaniotou, A. (2007). Agricultural residues as precursors for activated carbon production—A review. *Renewable and Sustainable Energy Reviews, 11*(9), 1966–2005.

Islam, M. A., Parvin, M. I., Dada, T. K., Kumar, R., & Antunes, E. (2024). Silver adsorption on biochar produced from spent coffee grounds: Validation by kinetic and isothermal modelling. *Biomass Conversion and Biorefinery, 14*(22), 28007–28021.

Johnson, K., Liu, Y., & Lu, M. (2022). A review of recent advances in spent coffee grounds upcycle technologies and practices. *Frontiers in Chemical Engineering, 4*, Article 838605.

Joshi, M., Srivastava, A., Bhatt, D., & Srivastava, P. C. (2023). Simple adsorptive removal of crystal violet, a triarylmethane dye, from synthetic wastewater using Fe (III)-treated pine needle biochar. *Environmental Monitoring and Assessment, 195*(4), Article 444.

Karmee, S. K. (2018). A spent coffee grounds based biorefinery for the production of biofuels, biopolymers, antioxidants and biocomposites. *Waste Management, 72*, 240–254.

Khezami, L., Taha, K. K., Ghiloufi, I., & El Mir, L. (2016). Adsorption and photocatalytic degradation of malachite green by vanadium doped zinc oxide nanoparticles. *Water Science and Technology, 73*(4), 881–889.

Lee, J. J. (2020). Adsorption characteristics of reactive red 120 by coal-based granular activated carbon: Isotherm, kinetic and thermodynamic parameters. *Applied Chemistry for Engineering, 31*(2), 164–171.

León, M., Silva, J., Carrasco, S., & Barrientos, N. (2020). Design, cost estimation and sensitivity analysis for a production process of activated carbon from waste nutshells by physical activation. *Processes, 8*(8), Article 945.

Lopes, C. D. C. A., Limirio, P. H. J. O., Novais, V. R., & Dechichi, P. (2018). Fourier transform infrared spectroscopy (FTIR) application chemical characterization of enamel, dentin and bone. *Applied Spectroscopy Reviews, 53*(9), 747–769.

Marrakchi, F., Ahmed, M. J., Khanday, W. A., Asif, M., & Hameed, B. H. (2017). Mesoporous-activated carbon prepared from chitosan flakes via single-step sodium hydroxide activation for the adsorption of methylene blue. *International Journal of Biological Macromolecules, 98*, 233–239.

Mata, T. M., Martins, A. A., & Caetano, N. S. (2018). Biorefinery approach for spent coffee grounds valorization. *Bioresource Technology, 247*, 1077–1084.

McNutt, J. (2019). Spent coffee grounds: A review on current utilization. *Journal of Industrial and Engineering Chemistry, 71*, 78–88.

Murthy, P. S., & Naidu, M. M. (2012). Sustainable management of coffee industry by-products and value addition—A review. *Resources, Conservation and Recycling, 66*, 45–58.

Na, C. (2020). Size-controlled capacity and isocapacity concentration in Freundlich adsorption. *ACS Omega, 5*(22), 13130–13135.

Nandiyanto, A. B. D., Oktiani, R., & Ragadhita, R. (2019). How to read and interpret FTIR spectroscope of organic material. *Indonesian Journal of Science and Technology, 4*(1), 97–118.

Ngueabouo, A. M. S., Tagne, R. F. T., Tchuifon, D. R. T., Fotsop, C. G., Tamo, A. K., & Anagho, S. G. (2022). Strategy for optimizing the synthesis and characterization of activated carbons obtained by chemical activation of coffee husk. *Materials Advances, 3*(22), 8361–8374.

Nogueira, G. A., Lopes, J. R., Vilas Boas, E. C., Cervantes, T. N., Moreira, A. B., Ferreira, O. P., & Bisinoti, M. C. (2025). Effect of the thermal activation on the adsorption capacity of cationic and anionic dyes in magnetic carbon. *ACS Omega, 10*(32), 36631–36643.

Ofomaja, A. E. (2008). Kinetic study and sorption mechanism of methylene blue and methyl violet onto mansonia (*Mansonia altissima*) wood sawdust. *Chemical Engineering Journal, 143*(1–3), 85–95.

Okpara, O. G., Ogbeide, O. M., Ike, O. C., Menechukwu, K. C., & Ejike, E. C. (2021). Optimum isotherm by linear and nonlinear regression methods for lead (II) ions adsorption from aqueous solutions using synthesized coconut shell–activated carbon (SCSAC). *Toxin Reviews, 40*(4), 901–914.

Ongen, A., Ozcan, H. K., Ozbas, E. E., & Balkaya, N. (2012). Adsorption of Astrazon Blue FGRL onto sepiolite from aqueous solutions. *Desalination and Water Treatment, 40*(1–3), 129–136.

Özbaş, E. E., Öngen, A., & Gökçe, C. E. (2013). Removal of astrazon red 6B from aqueous solution using waste tea and spent tea bag. *Desalination and Water Treatment, 51*(40–42), 7523–7535.

Özbaş, E. E., Balçık, B., & Ozcan, H. K. (2019). Preparation of activated carbon from waste tires, and its use for dye removal. *Desalination and Water Treatment, 172*, 78–85.

Phothong, K., Tangsathitkulchai, C., & Lawtae, P. (2021). The analysis of pore development and formation of surface functional groups in bamboo-based activated carbon during CO2 activation. *Molecules, 26*(18), 5641.

Prandini, M. N., Pranoto & Marliyana, S. D. (2022). A comparative study of kinetics of methylene blue dye using adsorbent andisol and humic acid from lighnite by KOH-hydrothermal method. *In Journal of Physics: Conference Series, 2190*(1), 012019.

Qiu, S., Qiu, T., Yan, H., Long, Q., Wu, H., Li, X., & Zhu, D. (2022). Investigation of protonation and deprotonation processes of kaolinite and its effect on the adsorption stability of rare earth elements. *Colloids and Surfaces a: Physicochemical and Engineering Aspects, 642*, Article 128596. https://doi.org/10.1016/j.colsurfa.2022.128596

Rodrigues, A. E., & Silva, C. M. (2016). What's wrong with Lagergreen pseudo first order model for adsorption kinetics? *Chemical Engineering Journal, 306*, 1138–1142.

Rudzinski, W., & Plazinski, W. (2007). Studies of the kinetics of solute adsorption at solid/solution interfaces: On the possibility of distinguishing between the diffusional and the surface reaction kinetic models by studying the pseudo-first-order kinetics. *The Journal of Physical Chemistry C, 111*(41), 15100–15110.

Rufián-Henares, J. A., & Pastoriza, S. (2015). Melanoidins in coffee. *Coffee in health and disease prevention* (pp. 183–188). Academic Press. https://www.sciencedirect.com/science/chapter/edited-volume/pii/B9780124095175000206

Sayğılı, H., & Güzel, F. (2018a). Uptake of anionic and cationic dyes by highly effective porous carbon adsorber based on industrial processing residues. *Separation Science and Technology, 53*(10), 1465–1475.

Sayğılı, H., & Güzel, F. (2018b). Behavior of mesoporous activated carbon used as a remover in Congo red adsorption process. *Water Science and Technology, 2017*(1), 170–183.

Setter, C., Borges, F. A., Cardoso, C. R., Mendes, R. F., & Oliveira, T. J. P. (2020). Energy quality of pellets produced from coffee residue: Characterization of the products obtained via slow pyrolysis. *Industrial Crops and Products, 154*, Article 112731.

Shah, H. H., Amin, M., Pepe, F., Mancusi, E., & Fareed, A. G. (2025). Overview of environmental and economic viability of activated carbons derived from waste biomass for adsorptive water treatment applications. *Environmental Science and Pollution Research, 32*(32), 19084–19109.

Sukhbaatar, B., Yoo, B., & Lim, J. H. (2021). Metal-free high-adsorption-capacity adsorbent derived from spent coffee grounds for methylene blue. *RSC Advances, 11*(9), 5118–5127.

Suteu, D., Zaharia, C., & Badeanu, M. (2016). Kinetic modeling of dye sorption from aqueous solutions onto apple seed powder. *Cellulose Chemistry and Technology, 50*, 1085–1091.

Tan, I. A. W., Ahmad, A. L., & Hameed, B. H. (2008). Adsorption of basic dye on high-surface-area activated carbon prepared from coconut husk: Equilibrium, kinetic and thermodynamic studies. *Journal of Hazardous Materials, 154*(1–3), 337–346.

Thenepalli, T., Ramakrishna, C., & Ahn, J. W. (2017). Environmental effect of the coffee waste and anti-microbial property of oyster shell waste treatment. *Journal of Energy Engineering, 26*(2), 39–49.

Tsai, W. T., Liu, S. C., & Hsieh, C. H. (2012). Preparation and fuel properties of biochars from the pyrolysis of exhausted coffee residue. *Journal of Analytical and Applied Pyrolysis, 93*, 63–67.

Wang, S., Zhu, Z. H., Coomes, A., Haghseresht, F., & Lu, G. Q. (2005). The physical and surface chemical characteristics of activated carbons and the adsorption of methylene blue from wastewater. *Journal of Colloid and Interface Science, 284*(2), 440–446.

Wang, C., Feng, X., Shang, S., Liu, H., Song, Z., & Zhang, H. (2023). Lignin/sodium alginate hydrogel for efficient removal of methylene blue. *International Journal of Biological Macromolecules, 237*, Article 124200.

Xia, X., Litvinov, S., & Muhler, M. (2006). Consistent approach to adsorption thermodynamics on heterogeneous surfaces using different empirical energy distribution models. *Langmuir, 22*(19), 8063–8070.

Yusufoğlu, B., Kezer, G., Wang, Y., Ziora, Z. M., & Esatbeyoglu, T. (2024). Bio-recycling of spent coffee grounds: Recent advances and potential applications. *Current Opinion in Food Science, 55*, Article 101111.

Zhang, S., Sun, X., Luo, Q., Chi, L., Sun, P., & Zhang, L. (2025). The Ce-modified biochar for efficient removal of methylene blue dye: Kinetics, isotherms and reusability studies. *Chinese Journal of Chemical Engineering, 77*, 57–65.

Publisher's Note Springer Nature remains neutral with regard to jurisdictional claims in published maps and institutional affiliations.